Characterizing Some of the Influences of the General Circulation on Subtropical Marine Boundary Layer Clouds

MARGARET A. ROZENDAAL

Program in Earth and Environmental Sciences, Columbia University, New York, New York

WILLIAM B. ROSSOW

NASA Goddard Institute for Space Studies, New York, New York

(Manuscript received 27 February 2001, in final form 3 September 2002)

ABSTRACT

The seasonal and intraseasonal variability of boundary layer cloud in the subtropical eastern oceans is studied using combined data from the International Satellite Cloud Climatology Project and the European Centre for Medium-Range Weather Forecasts reanalysis.

Spectral analysis reveals that most of the time variability of cloud properties occurs on seasonal to annual timescales. The variance decreases by one to two orders of magnitude for each decade of timescale decrease, indicating that daily to monthly timescales and their spatial extent have smaller, although nonnegligible, variability. The length of these dominant timescales suggests that the majority of the variability is influenced by the general circulation and its interaction with boundary layer turbulence, rather than being a product of local boundary layer turbulence alone. Although the dominance of seasonal to annual periods in the temporal power spectra of low-cloud fraction—TAU and CTP—justifies the previous focus of effort on seasonal variability, intraseasonal data can be better used to examine the cloud formation/dissipation processes as revealed in relationships between synoptic meteorology and cloud properties.

Previous datasets have lacked the necessary combination of resolution and scope in either time or space coverage to properly characterize variability on synoptic and larger scales; this is remedied by using global satellite-retrieved cloud properties. The intraseasonal subtropical cloud variability in both hemispheres and in different seasons are characterized. In addition to cloud fraction, variability of cloud optical thickness and cloud-top pressure frequency distributions are examined.

The intraseasonal variability is divided into three types. The first type, found in the Californian local summer and Southern Hemisphere regions year round, is characterized by lower-altitude, greater optical thickness, stationary clouds. The second type is found in the Canarian local summer and has more instances of smaller cloud-top pressures and a westward propagation direction. The third type, found in Northern Hemisphere regions during winter, is similar to the second type, but shows an eastward propagation direction. This study focuses on the third type more closely and finds it to be associated with the lower sea level pressure, upward vertical velocity phase of synoptic waves.

1. Introduction

Recent model studies have examined the consequences of deficiencies in the representation of subtropical low cloud on the coupling between the ocean and the atmosphere. Several of these experiments (Ma et al. 1996; Yu and Mechoso 1999; Gordon et al. 2000; Li et al. 2000) artificially increase low-cloud fraction, persistence, or optical thickness to study its effect on the radiation balance and SST of the eastern equatorial Pacific and the subsequent dynamic response. Such changes in the low clouds resulted in improvements such as larger, and more realistic, latitudinal and longitudinal SST asymmetries, larger surface wind speeds, and increased surface evaporation in the marine stratus regions.

Understanding the reasons behind GCM subtropical cloud deficiencies and their interactions with the large-scale circulation requires a more detailed examination of the time variability of cloud properties in both models and data. However, comparisons between cloud properties from GCMs and data have concentrated primarily on seasonal averages; the lack of shorter timescale information makes it difficult to identify sources of model deficiencies. For instance, some GCMs underestimate seasonal mean subtropical low-cloud fraction by 10%–30% compared to surface observations (Del Genio et al. 1996; Ma et al. 1996) and the International Satellite Cloud Climatology Project (ISCCP; Jakob 1999); but

Corresponding author address: Dr. William B. Rossow, NASA GISS, 2880 Broadway, New York, NY 10025.
E-mail: wrossow@giss.nasa.gov

based on this information alone, it is impossible to determine whether this deficiency is due to a difference in frequency of occurrence or amount of coverage, let alone to diagnose relationships between variations in the general circulation, cloud processes, and cloud properties. Only very recently have cloud properties from GCMs and datasets been compared on the daily timescale (e.g., Webb et al. 2001).

The next step would seem to be to use smaller-scale models (e.g., single-column, large eddy simulation, and cloud resolving models) under varying large-scale boundary conditions to investigate changes in the cloud processes. Unfortunately, these models require extensive information to constrain their boundaries. Therefore, studies using them have tended to focus on the simpler problem of simulating locally, horizontally homogeneous regions during periods where the boundary conditions remain approximately steady. Under these constraints, the emphasis of most smaller-scale modeling studies has been on the role of boundary layer turbulence in the formation and dissipation of these clouds. In these cases, models generally simulate time periods of hours to days with fixed large-scale parameters [Moeng et al. (1996) and Bechtold et al. (1996) provide intercomparisons of some state-of-the-art smaller-scale models]. For example, Weaver and Pearson (1990) summarizes these studies as concentrating on identifying a thermodynamic (i.e., local) criterion for cloud breakup in contrast to examining variations caused by large-scale dynamics.

What is the current state of our understanding of cloud variability from data? Until recently, datasets have suffered either from a lack of temporal resolution and coverage, or a lack of spatial coverage or both. Global studies of low-cloud time variability and the general circulation have focused mainly on seasonal mean properties (Klein and Hartmann 1993, hereafter KH93; Tselioudis et al. 1992) or seasonal variability of the diurnal cycle (Cairns 1995; Rozendaal et al. 1995; Bergman and Salby 1996). We have not yet addressed such basic questions as regards the most important time- and space scales of variability of subtropical marine boundary layer clouds, and whether or not the characteristics of this variability are similar for all subtropical regions.

Studies of the time variability of marine low-level clouds at smaller spatial scales (summarized in Klein 1997) have been restricted to the Northern Hemisphere (NH) regions during summer, with most of the emphasis on the more frequently observed Californian region. In addition, many of these studies are limited to the examination of low-cloud fraction only. The types of variability studied include daily to monthly timescales in the Californian region (Klein 1997), the diurnal cycle (Simon 1977; Betts 1990; Blaskovic et al. 1991; Bretherton et al. 1995), and time variability in the vertical structure (Albrecht et al. 1995a; Norris 1998; Wang et al. 1999). However, these data cannot be used to examine the interactions of large-scale meteorology and clouds or to compare multiple regions during the same time period because they are restricted in the spatial scales covered. Weaver and Pearson (1990) combines satellite images and weather analysis (noting the lack of actual meteorological data) to examine a few cases of synoptic variations.

In summary, we emphasize several points. First, coupled atmosphere–ocean GCM studies note that misrepresenting these clouds and their effect on the surface radiation balance causes incorrect dynamic coupling between the atmosphere and the ocean. This deficiency casts doubt on our ability to correctly account for the effects of cloud variability in predictions of long-range weather and climate change. However, with the emphasis on comparing seasonal mean values, it has been difficult to identify and isolate model deficiencies. Second, despite the importance of this problem, smaller-scale modeling investigations have not addressed the effects of large-scale variability on cloud processes. What is missing are modeling studies that bridge the gap between the static large-scale forcing studies of the smaller-scale models and the GCM studies where all large- and small-scale processes vary and interact simultaneously. Third, the lack of long-term, larger-spatial-scale observations that resolve the time variability of clouds on small and large scales, together with the large-scale atmosphere, has prevented an observational attack on this problem.

Our contributions to these problems are as follows. After describing the datasets, the model reanalysis product, and the details of some data analysis techniques used in this study, in section 2, we use the ISCCP dataset to characterize the whole range of time variations of marine subtropical low-cloud properties, extending this characterization beyond cloud cover fraction to include cloud-top pressure and optical thickness (section 3). Time variability spectra are shown and the seasonal cycle and synoptic (defined here as roughly 3–10 days) variability are identified as the two most important scales of time variability. We examine the seasonal and intraseasonal variability for four subtropical regions and note that the characteristics are not the same, so they cannot be explained by a single model. Section 4 examines relationships between variability in cloud properties and the general circulation. In particular, we focus on the NH wintertime variability. To do this, we combine satellite-retrieved cloud data with the reanalysis product of an atmospheric model (observations interpolated by model output). Using this combination of information enables us to generalize results for all regions rather than focusing on a particular local case study.

2. Data

a. Satellite data

Nine years (1984–92) of data obtained from the ISCCP D-series (Rossow et al. 1996; Rossow and Schif-

TABLE 1. Boundaries of the 10° × 10° regions for the Californian (CAL), Peruvian (PER), Canarian (CAN), and Namibian (NAM) locations. Other sizes are concentric around the given boundaries. The 2.5° × 2.5° region is the box most equatorward and westward within the 5° × 5° region. The Canarian region is shifted 5° west from KH93 to avoid coastal influences.

Region	Lat	Lon
CAL	20°–30°N	120°–130°W
PER	10°–20°S	80°–90°W
CAN	15°–25°N	20°–30°W
NAM	10°–20°S	0°–10°E

fer 1999) are used in this analysis. The distribution of cloud properties are provided at spatial intervals of 280 km (approximately 2.5°) and time intervals of 3 h for the D1 and monthly for the D2 dataset. Since the best cloud information is obtained when both visible (VIS) and infrared (IR) wavelength measurements are available, daily averages are calculated using these hours only. Since the maximum and/or minimum values do not always occur during the daytime hours, linear interpolation over the nighttime hours would not remove potential biases. Biases and other errors in ISCCP VIS/IR cloud-top temperature and cloud fraction are discussed at length in Wang et al. (1999).

This study characterizes low clouds by examining the variability of cloud fraction, cloud optical thickness (TAU), and cloud-top pressure (CTP). Low-cloud is defined in ISCCP as having CTP $>$ 680 mb. We refer to all other clouds with CTP $<$ 680 mb (middle- plus high-level cloud) as upper-level clouds. Most of the results are presented for 10° × 10° domain sizes (boundaries given in Table 1); but results for other domain sizes are included as necessary.

To be consistent with previous studies (e.g., Lau and Crane 1995, 1997; Tselioudis et al. 2000), TAU is used to describe cloud water changes rather than cloud liquid water path (LWP). However, these two variables are directly related at the smallest (pixel) scale for ISCCP water clouds by the relationship LWP = TAU × 6.292 × 10^{-3}, where LWP is in kilograms per square meter, when the effective droplet radius is 10 μm, (Rossow et al. 1996). A more detailed discussion of the relationship between these two variables can be found in Han et al. (1998). All analyses in this paper have been made using both variables; using LWP rather than TAU would not change our conclusions.

Although we generally use CTP to study variations in cloud-top location, all tests in this paper were also performed using cloud-top temperature and cloud-top height [where cloud-top height is estimated as the difference between cloud-top and surface temperatures divided by a fixed lapse rate of 6.5 K km^{-1} (e.g., Salby 1996)]. The conclusions would be the same with these other quantities so, unless otherwise noted, CTP is used as a proxy for either of these two variables.

The ISCCP dataset also includes atmospheric temperature information provided by the *Television Infrared Observational Satellite* (*TIROS*) Operational Vertical Sounder (TOVS) product processed by the National Oceanic and Atmospheric Administration (NOAA) National Environmental Satellite, Data, and Information Service (NESDIS). Static stability is calculated as the difference between the potential temperature at 740 mb (θ_{740}) and the surface temperature; θ_{740} is calculated using the TOVS atmospheric temperature. Although a near-surface temperature is also available from TOVS, according to Fig. 11 of Stubenrauch et al. (1999), TOVS temperatures over these regions tend to run approximately 2 K colder at the surface and 0–1 K warmer at 740 mb, compared to temperatures processed using the improved initialization inversion (3I) algorithm. Therefore, we try to minimize this systematic error by using the mean surface skin temperature from the ISCCP clear-sky composite to represent the surface temperature (Rossow et al. 1996; Rossow and Schiffer 1999).

b. ERA-15 model product

Meteorological variables are provided by the European Centre for Medium-Range Weather Forecasts (ECMWF) Reanalysis level III-B surface and upper air data for 1979–93 (known as ERA-15, hereafter ERA). We extract model products for the same time and at the same spatial resolution as the ISCCP data, except that daily averages are calculated using 6-hourly model data.

This study uses ERA sea level pressure (SLP) from the surface dataset, plus temperature (T), and vertical pressure velocity (ω) at various pressure levels indicated by a subscript (for instance, ω_{700} is the vertical pressure velocity at 700 mb). ERA static stability is calculated as the difference between potential temperatures at 700 and 1000 mb ($\theta_{700} - \theta_{1000}$). The meridional change in any variable across the region is estimated as the difference between the most equatorward and most poleward boxes ($X_{\text{eq}} - X_{\text{pole}}$) within the 10° × 10° domain, at the longitude farthest away from the coast. The subscript "v" is used to designate meridional changes, for instance, "Δ_vSLP" represents the meridional change in SLP across the domain.

c. Ocean weather station sounding data

This study also uses upper air data from ocean weather stations (OWSs) N (30°N, 140°W) and P (50°N, 130°W). We limit the data to the nighttime hours due to daytime biases in temperature and relative humidity (e.g., Klein 1997; Norris 1998). Sounding data are available for the years of 1949–74 for OWS N and 1949–70 for OWS P. These soundings provide vertical profiles of pressure, height, temperature and relative humidity at 50-mb intervals. We use the relationships outlined in Bolton (1980) to convert the data to water vapor mixing ratio (q), potential temperature (θ), and equivalent potential temperature (θ_e) as necessary.

We identify the pressure and temperature associated

with the base of the temperature inversion using the method described in Klein (1997). Since the temperature inversion is associated with a rapid increase in temperature and decrease in relative humidity with height, these differences are calculated for each 50-mb layer. However, since these changes can occur in layers less than 50 mb in thickness, the inversion structure may not appear explicitly in these coarse resolution soundings. Instead, it is assumed that the layer containing the inversion will show the smallest fall in temperature and the largest decrease in relative humidity with height. If these changes occur in the same layer, then the base of the trade inversion is marked as the pressure at the base of this 50-mb layer. Soundings that do not meet both of these criteria are discarded from the analysis.

d. Data compositing method

Following earlier studies of this kind (Klein et al. 1995; Klein 1997; Lau and Crane 1995, 1997; Tselioudis et al. 2000; Norris and Klein 2000), we composite ISCCP cloud properties in categories based on anomalies in meteorological data from ERA. In particular, we follow the method of Tselioudis et al. (2000), who use 12-hourly SLP anomalies to identify the passage of low pressure systems and to group clouds by synoptic regime.

To separate time variability from spatial variability, the data are spatially averaged over $10^\circ \times 10^\circ$ regions on each day (the general observations based on frequency distributions shown in this paper did not change whether the domain size was increased to $20^\circ \times 20^\circ$ or reduced to a single $2.5^\circ \times 2.5^\circ$ box within the larger domain). Anomalies in ERA and TOVS meteorology are calculated by subtracting monthly means from daily averages. To summarize seasonal differences found in a more detailed analysis, anomalies for the months of May–September (MJJAS) and November–March (NDJFM) are collected together and are referred to as ''seasonal anomalies'' for the remainder of this paper (although we primarily discuss the results for NDJFM in this paper, results for both seasons are calculated). For each season, the resulting anomalies are separated into positive and negative groups and the median value is calculated for each group. All of the anomalies, and their associated cloud properties, are then resorted into three groups: anomalies larger than the positive median (POS ANOM), anomalies less than the negative median (NEG ANOM), and anomalies larger than the negative median, but smaller than the positive one (ZERO ANOM; see Fig. 1 of Tselioudis et al. 2000 for an illustration). When discussing CTP–TAU frequency distributions, we refer to the six TAU classes and seven CTP classes defined in Fig. 2.5 of Rossow et al. (1996) and used by Tselioudis et al. (2000).

3. Characterizing large-scale subtropical cloud variability

a. Variability spectrum

Using four of the subtropical domains chosen by KH93 (Table 1), we calculate the power spectra for time variations of TAU, CTP, and cloud fraction. This spectral method (Press 1992) uses five overlapping windows with 512 days in each window (the method requires the window size to be a power of two). The power spectrum for low-cloud TAU in Fig. 1 shows the dominance of seasonal to annual timescales in cloud variability (the spectra for cloud fraction and CTP are similar and therefore not shown). The spectra for total cloud variables, in particular cloud fraction, show a larger concentration of power at synoptic timescales. The spectrum is clearly ''red'' (e.g., Gilman et al. 1963), so most of the variance occurs at longer time periods. Figure 1 also shows that the spectral slope changes just above and below the synoptic timescale range, which indicates a relative deficit of energy just above the synoptic timescales and a relative excess at synoptic scales. These variations in slope are significant because spectra created by taking subsets of the data all produce the same result (not shown). The existence of the plateau indicates that all of the power at daily to monthly timescales cannot be explained by nonlinear cascades either from longer or shorter timescales, requiring a source of energy near these timescales. As both the temporal and spatial spectra (e.g., Pandolfo 1993; Rossow and Cairns 1995) are red in character, this is indicative of the longer timescales being associated with larger spatial scales. The magnitude of the dominant timescales suggests that the majority of the cloud variability is controlled by the general circulation and its interaction with boundary layer turbulence, rather than the product of local boundary layer changes alone.

Using a cutoff of $1/e \sim 0.37$ for the autocorrelation, the decorrelation timescale for total cloud TAU, CTP, and cloud fraction is about 3 days in all $10^\circ \times 10^\circ$ regions (since the data are daily averages, there is no spectral information for periods less than the Nyquist frequency of 2 days). Studies at higher spatial resolution show that the spatial power spectrum for stratocumulus clouds continues to follow a power-law relationship (Welch et al. 1988; Sengupta et al. 1990) and that the magnitude of cloud variations at scales smaller than approximately 5 km contributes little to the total cloud variability (Barker 1996; Chambers et al. 1997). These results and the negative slopes of both the time and spatial power spectra argue that the variance continues to decrease at timescales shorter than 2 days. Using Atlantic Stratocumulus Transition Experiment (ASTEX) data, Wang et al. (1999) show that, even for the diurnal cycle, the variance is half that of synoptic timescales (their Table 2). This is consistent with time spectra shown by Rossow and Cairns (1995) and kinetic energy spectra from Fig. 2.4 of Peixoto and Oort (1992). There-

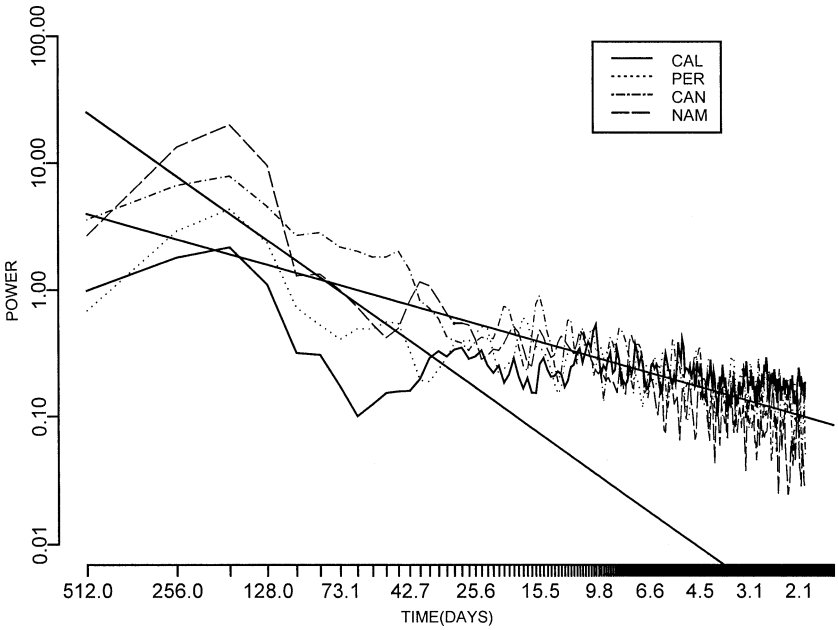

FIG. 1. Temporal spectrum of daily average ISCCP low-cloud TAU on the 10° × 10° spatial scale for 9 yr (1984–92) for the four regions of Table 1. Two lines representing power laws with exponents −2/3 and −5/3 are shown for reference.

fore, there is more power at the few-days to seasonal timescales than at the hourly to daily timescales characteristic of boundary layer turbulence.

We tested the dependence of spectral shape on changes in the size of the averaging domain, latitude and longitude regions, and seasonal definition (months included). As the domain size increases from 2.5° × 2.5° to 20° × 20°, more power is found at seasonal to annual timescales and less at intraseasonal. This is not unexpected since shorter period variability is smoothed by spatial averaging as the domain size increases. Varying the location of the 2.5° × 2.5° boxes within the larger 20° × 20° domain causes small changes in power at the seasonal frequencies and slight changes in slope between the seasonal and intraseasonal frequencies. However, no major differences in spectral shape were noted. If the spectrum is calculated for MJJAS and NDJFM separately, the NH regions exhibit some changes in shape with season. During NDJFM, there is an increase in power at intraseasonal timescales for periods less than 30 days and a decrease in the slope between seasonal and intraseasonal timescales. In contrast, the Southern Hemisphere (SH) regions show no significant changes in power or spectral shape with season. The differences in variability between hemispheres will be explored in later sections.

b. Seasonal variability

We extend previous studies of the seasonal variation of low-cloud fraction to include variations in ISCCP TAU and CTP (Table 2). Although some of these results have been shown elsewhere (e.g., KH93; Randall et al. 1996), a brief discussion is included here as we attempt to characterize similarities and differences among these four regions. As noted in earlier papers (e.g., Schubert et al. 1979; KH93), seasonally averaged low-cloud fraction is larger during MJJAS than NDJFM in all of these eastern ocean subtropical regions, regardless of whether the local season is summer or winter. The MJJAS upper-level cloud fraction is small, around 10%, with most of the coverage by middle-level cloud. Therefore, the possibility of obscuration of low-level cloud by upper-level cloud is rare during this season.

When subdivided by cloud type, most of the low cloud falls into the ''stratocumulus'' (Sc) TAU category, in the range of 3.6 to 23.3 (Rossow et al. 1996): 70%–75% of the VIS/IR low-cloud fraction is Sc and 17%–25% cumulus (Cu), with smaller amounts of stratus (St) in all regions except the Canarian. The low-cloud fraction in the Canarian region is comprised of almost equal parts Sc and Cu. These differences in low-cloud fraction amount and type among the subtropical regions are in qualitative agreement with seasonally averaged surface observations from the dataset of Warren et al. (1988), despite differences in the definition of these cloud types for each dataset. Hahn et al. (2001) provide a comprehensive discussion of the extent to which ISCCP clouds are associated with standard surface observer cloud types. To summarize, ISCCP cannot distinguish between Cu, Sc, and St cloud types in *individual* observations because of the considerable overlap in the CTP–TAU distributions associated with each of these cloud types. However, changes in ISCCP TAU distributions resemble

TABLE 2. ISCCP D2 VIS/IR (1984–92) seasonal averages and differences for cloud fraction (%), TAU, and CTP (mb). Cloud information is separated into low-level (low) and total cloud types as defined by ISCCP. Cloud fractions associated with St, Sc, and Cu optical thicknesses are also included.

	Low						Total		
Region	CF	St CF	Sc CF	Cu CF	TAU	CTP	CF	TAU	CTP
MJJAS									
CAL	65.4	7.8	45.0	12.6	8.9	800	81.8	8.1	755
PER	65.9	2.3	46.4	17.2	4.9	785	81.6	10.6	750
CAN	43.1	1.1	21.0	21.0	2.4	845	60.8	3.6	735
NAM	66.2	4.2	49.0	13.0	6.8	810	78.2	8.4	765
NDJFM									
CAL	45.7	1.9	27.0	16.8	3.0	805	79.6	5.6	675
PER	48.0	3.8	31.0	13.2	5.8	775	66.5	6.6	715
CAN	34.2	0.8	12.3	21.1	1.5	850	64.9	3.4	685
NAM	57.8	3.8	43.3	10.7	7.1	815	70.4	7.9	750
MJJAS–NDJFM									
CAL	19.7	5.9	17.9	−4.1	5.0	−5	2.2	2.5	80
PER	17.9	−1.5	15.4	4.0	−0.9	10	15.1	4.0	35
CAN	8.9	0.3	8.7	−21.1	0.9	−5	−4.1	0.2	50
NAM	8.4	0.4	5.9	−0.6	−0.3	−5	7.8	1.5	15

expected changes in surface-observed cloud type when surface observations are composited into spatial and seasonal averages. Therefore, in this section, we treat surface-observed and ISCCP cloud types as though they are equivalent; but in later sections, when we examine distributions of daily averaged data, we refer to clouds of different TAU as ''thinner'' and ''thicker'' clouds.

During NDJFM, low-cloud fraction decreases in all regions relative to the MJJAS values. This is primarily a decrease in Sc type cloud fraction; changes in Cu and St cloud fractions are of mixed sign. Part of this decrease may be caused by an increase in obscuration by upper-level cloudiness, but (with the exception of the Canarian region) low-cloud fraction decreases are larger than increases in upper-level cloudiness. From these data alone, it is impossible to determine the extent to which upper-level clouds replace or obscure low-level clouds [although Figs. 6 and 7 of Jin and Rossow (1997) show increases in multilayer cloud coverage during NDJFM, suggesting that low clouds may be obscured rather than replaced]. However, this seasonal decrease of low-cloud fraction is also consistent with results from the dataset of Warren et al. (1988). In this case, the surface-observed decrease in low-cloud fraction is the result of decreases in both amount-when-present and frequency-of-occurrence of St and Sc cloud types, and an increase in the frequency-of-occurrence of Cu.

Low-cloud TAU and CTP are estimated for the low clouds that are seen. The relationship between seasonal variations in TAU and atmospheric temperature appears to be inconsistent with Tselioudis et al. (1992) since, for all regions, low-cloud TAU is larger during the locally warmer season. However, as pointed out in their paper, this relationship is not particularly robust for this cloud type and averaging over 8 yr of data, as well as several months of the year, includes time periods where the relationship changes sign. In addition, we only consider a portion of the eastern ocean while Tselioudis et al. aggregate over all longitudes. If we subdivide the low-cloud TAU by cloud type, in the NH regions TAU values are much larger for the St cloud type in NDJFM and slightly larger for Sc and Cu types in MJJAS (not shown). Therefore, as the NH season changes from warmer to cooler, thicker clouds increase in thickness while thinner clouds become thinner. This is more consistent with Tselioudis et al., however, since the coverage by St type clouds is such a small fraction of the total, this effect is lost when considering the average low-cloud TAU.

For all of these subtropical regions, total cloud CTP is smaller during NDJFM than MJJAS (Table 2). The low-cloud CTP differences during the same seasonal transition are mixed; however, as the seasonal differences in low-cloud CTP are all very small (5–10 mb), this small amplitude variability may not be reliably detected or may not be significant.

The main point that results from this analysis is that the seasonal cloud variability is not the same for all subtropical cloud regions. Therefore, looking for a single theory or local relationship to explain the variability will not accommodate all of the results. For instance, many studies have examined the subtropical cloud variations as the result of changes in tropical convection (e.g., Sarachik 1978; Betts and Ridgway 1989; Miller 1997; Clement and Seager 1999; Larson et al. 1999). However, this type of one-way relationship that does not consider the feedback of the cloud changes on the large-scale circulation may not be able to consistently explain the seasonal cycle. A fully interactive study is needed.

c. Intraseasonal variability

Although the dominance of seasonal to annual periods in the temporal power spectra of low-cloud fraction,

TABLE 3. Number of times low-cloud fraction surpasses the threshold cloud fraction during each season (1984–92).

Threshold region	>70%		>50%	
	MJJAS	NDJFM	MJJAS	NDJFM
CAL	95	56	82	92
PER	75	36	109	85
CAN	13	16	60	54
NAM	78	67	103	94

TAU and CTP justifies the previous focus of effort on seasonal variability, intraseasonal data can be better used to examine the cloud formation/dissipation processes as revealed in relationships between synoptic meteorology and cloud properties. Time–longitude Hovmöller diagrams of low-cloud fraction at latitudes of 25°–30°N (not shown) over the eastern Pacific Ocean show fairly stationary and persistent large low-cloud fraction events from approximately May to September. These events are not regularly spaced in time nor do they persist for the same length of time. Similar variability is seen in diagrams at the latitude of the Peruvian and Namibian regions. However, as also noted in KH93, the initiation of a season of large low-cloud fraction events in these regions lags behind the Californian by 1 to 2 months.

During this same season, the characteristics of cloud properties in the Canarian region are different from the other three subtropical regions. Time–longitude diagrams of all cloud properties, but particularly CTP (not shown), indicates that upper-level cloud events propagate from east to west at estimated speeds of 10 m s^{-1} and, by obscuring or replacing the lower-level clouds, shorten the perceived low-cloud persistence observed from satellites.

For the other months of the year, the persistence and propagation characteristics of the synoptic variability change. In the SH, large low-cloud fraction events decrease in both magnitude and frequency, but are still stationary. In the NH regions, the persistence and frequency of occurrence of large low-cloud fraction events resembles the Canarian MJJAS variability, except that the upper-level cloud events propagate in the other direction, from west to east.

We quantify these observations by counting the number of times the low-cloud fraction exceeds a chosen threshold value, and once it does, how many days it remains above this value. For a threshold value of 70%, Table 3 shows that large low-cloud fraction events occur more frequently during MJJAS in all regions except the Canarian. This exception occurs because the low-cloud fraction in the Canarian region seldom reaches 70%, but the same result is achieved there when the threshold value is reduced to 50%. Figure 2 shows that the fre-

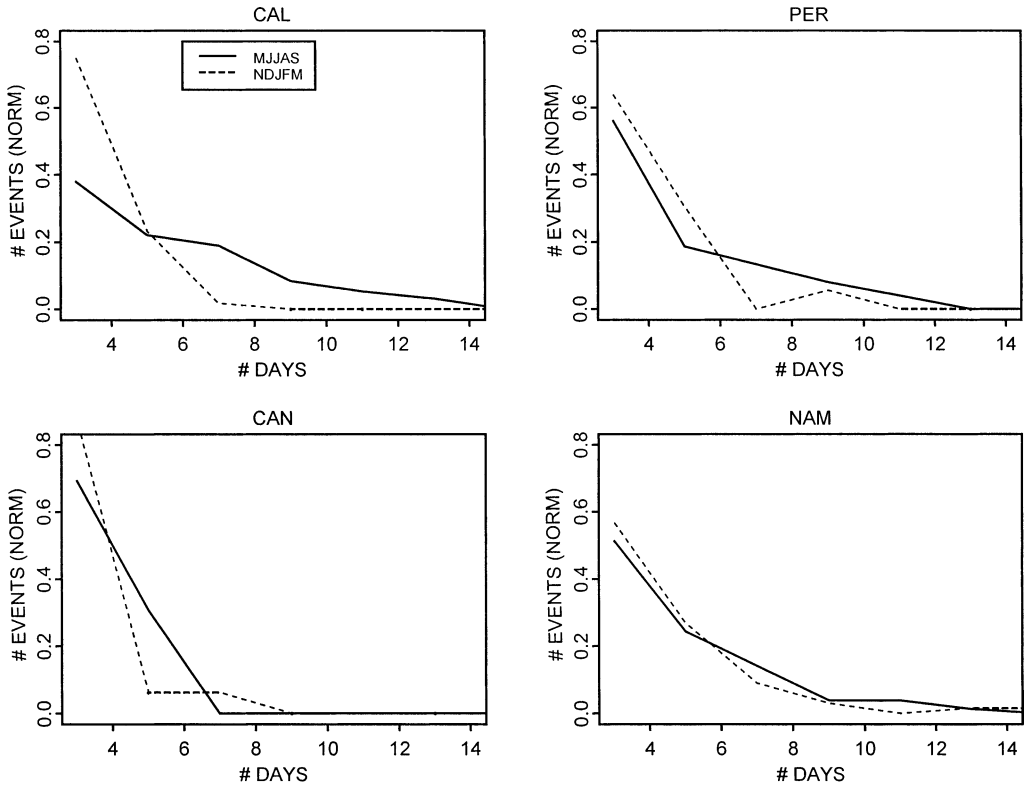

FIG. 2. Persistence (days) of low-cloud fraction events larger than 70% during MJJAS and NDJFM (1984–92). Distributions are normalized by the total number of events for that season.

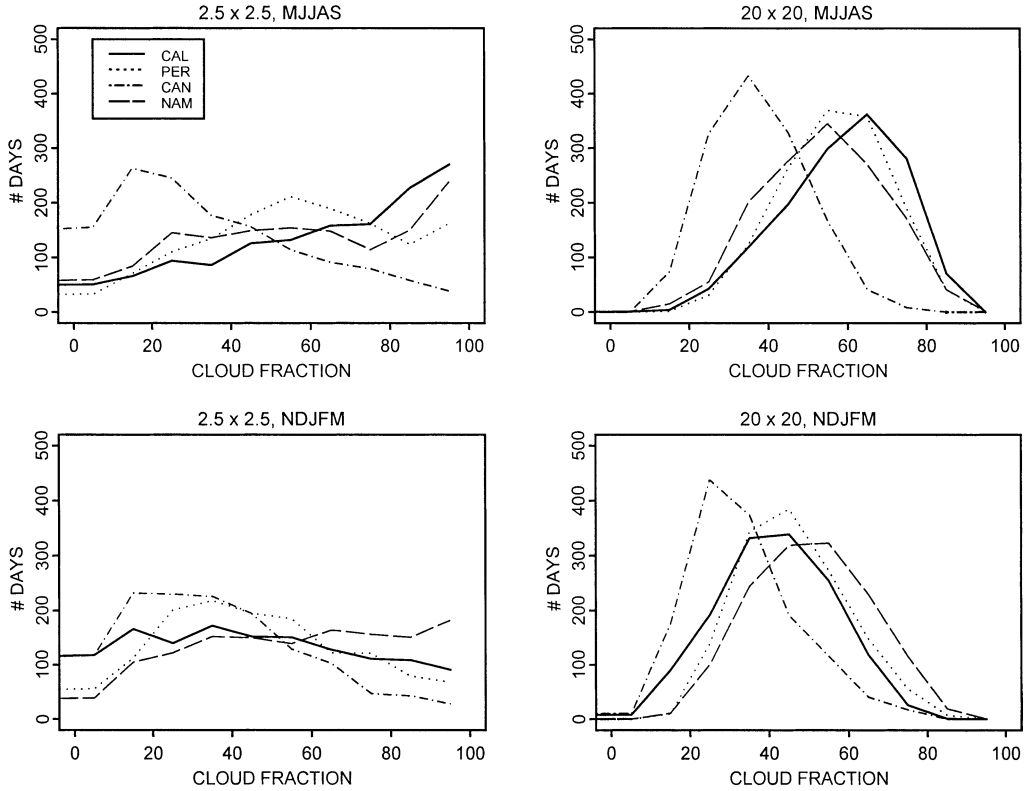

FIG. 3. Frequency distributions of daily average ISCCP low-cloud fraction (1984–92) on 2.5° × 2.5° and 20° × 20° spatial scales for MJJAS and NDJFM.

quency of occurrence of these large events is greater in the NH regions during the MJJAS season, while in the SH regions large persistent events still occur during the NDJFM season, although with less frequency in the Peruvian case. Together, we find that the observed seasonal differences in low-cloud fraction are due primarily to changes in the mean values in the SH and to changes in frequency of occurrence and persistence in the NH.

Although the seasonal average is a commonly reported statistic, other characteristics of a distribution are often more informative, particularly if the distribution shape is not normal. For low-cloud fraction (Fig. 3) and total cloud fraction (not shown) the shape of the frequency distribution varies with domain size. At the 2.5° × 2.5° spatial scale, the distributions have a wide range of mode values, varying from 20% in the Canarian region to nearly overcast in the Namibian. The mode values converge to approximately 60% and the shape of the distribution approaches near normal as the domain size increases to 20° × 20°. This is consistent with observations of Rossow and Cairns (1995) and Klein (1997) for subtropical surface observations. Both demonstrate that the cloud fraction frequency distribution is dominated by completely overcast or clear-sky cases at smaller spatial scales, but the mode value approaches ''partly cloudy'' as the domain size increases. Therefore, the seasonally averaged low-cloud fraction shown in Table 2 could potentially mask different types of intraseasonal variability.

In contrast to cloud fraction, frequency distributions for total cloud TAU (Fig. 4) and CTP (not shown) exhibit little variation in shape or mode when changing the averaging domain size. These distributions are monomodal, with the distribution becoming narrower as the domain size increases. The comparison of Figs. 3 and 4 illustrate a method of characterizing low-cloud variability which removes the bias of domain size on the resulting statistics.

Figure 5 characterizes subtropical clouds using a two-dimensional frequency distribution of cloud TAU and CTP for the 10° × 10° domain (results are similar on all spatial scales). During MJJAS, the Californian distribution looks more like the SH distributions, with primarily low-altitude cloud tops and a broad range of TAU values. Cloud properties in the Canarian region are distributed differently, with more frequently occurring high-altitude cloud tops and smaller TAU values. As the season shifts from MJJAS to NDJFM, the most drastic change in cloud properties occurs in the Californian region, where the frequency of occurrence increases for higher-altitude clouds and decreases for larger TAU clouds.

At this point, low-cloud variability can be separated into three distinct types. The first type occurs in the SH

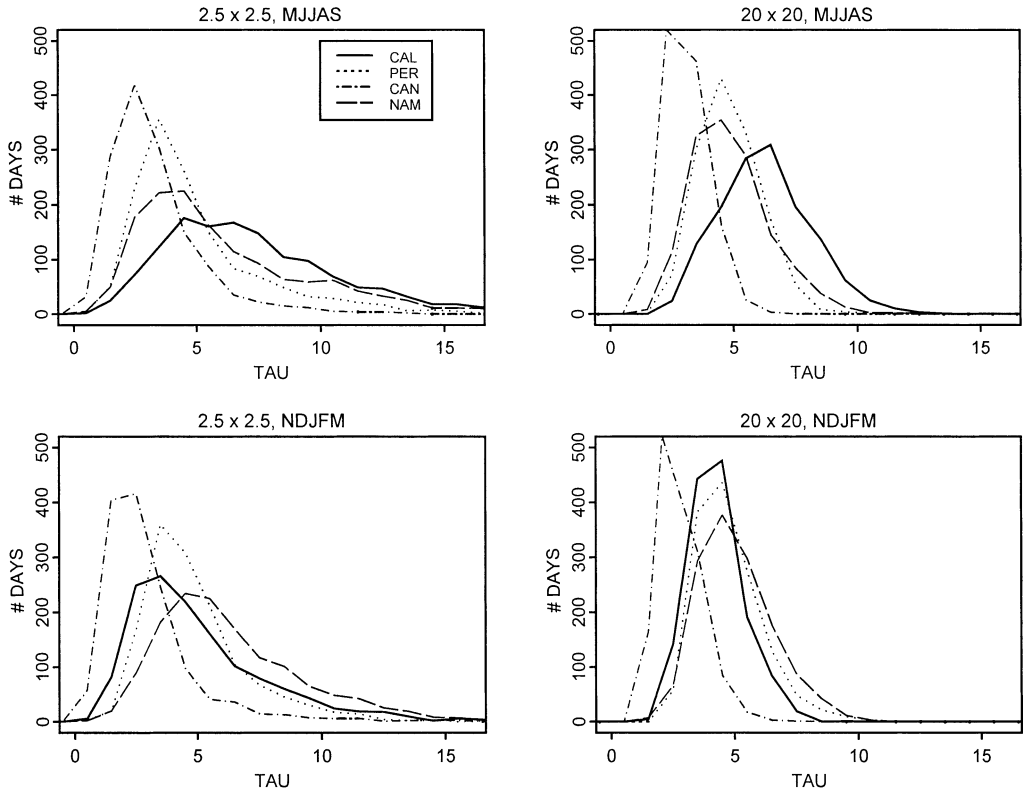

FIG. 4. Same as Fig. 3, but for ISCCP total cloud TAU.

regions during *both* seasons, and in the Californian region during local summer. In this case, subtropical low clouds vary more in TAU than in CTP. This variability generally occurs on timescales longer than the 10-day upper bound of synoptic variability. The second type of variability is found in the Canarian region during local summer. The CTP–TAU characteristics are similar to the ranges found in the local winter season, but Hovmöller diagrams indicate a westward direction of propagation rather than eastward. The third type is found in the NH regions during local winter. In this case, the CTP shows a large range of variability, while TAU variability is relatively small. Hovmöller diagrams show that this CTP variability is associated with an eastward direction of propagation. These results have several implications. They demonstrate that seasonal averages should be interpreted with caution since they mask important differences in intraseasonal variability. They also imply that the causes of cloud variability for all the subtropical regions are not the same, so these regions cannot be treated interchangeably.

How do the large-scale conditions change and alter the physical processes that control low-cloud variability? In the first case, the longer-period variability could be controlled by changes in tropical convection. The second type of variability (Canarian summer) is similar to tropical variability noted by Chang (1970) and Cho and Ogura (1974); it could be the result of easterly waves originating on the African continent, with wavelengths of approximately 2500 km and periods of about 3–4 days (e.g., Carlson 1969; Burpee 1972; Reed et al. 1977). The third type of variability (NH regions during local winter) could be due to the influence of wintertime midlatitude synoptic storms. In this case, it is significant that the NH regions are located more poleward than their SH counterparts (see Table 1). This latitudinal difference, combined with an equatorward shift in NH storm-track activity during the NH winter season (Trenberth 1991; Rossow et al. 1993), allows midlatitude storms to intrude into the NH subtropical regions. In contrast, the SH regions do not show this change in variability since the storm track is located at approximately 45°S all year round, keeping the storms poleward of the subtropical stratiform cloud regions. A full examination of all three mechanisms, requiring a combination of data analysis and cloud-resolving modeling studies with large-scale boundary conditions, is beyond the scope of this paper. However, we examine in more detail one of the mechanisms, the encroachment of midlatitude storms into the subtropics during NH winter, as an example of the types of interactions between large-scale dynamics and boundary layer processes that produce the intraseasonal variability in cloud properties presented here.

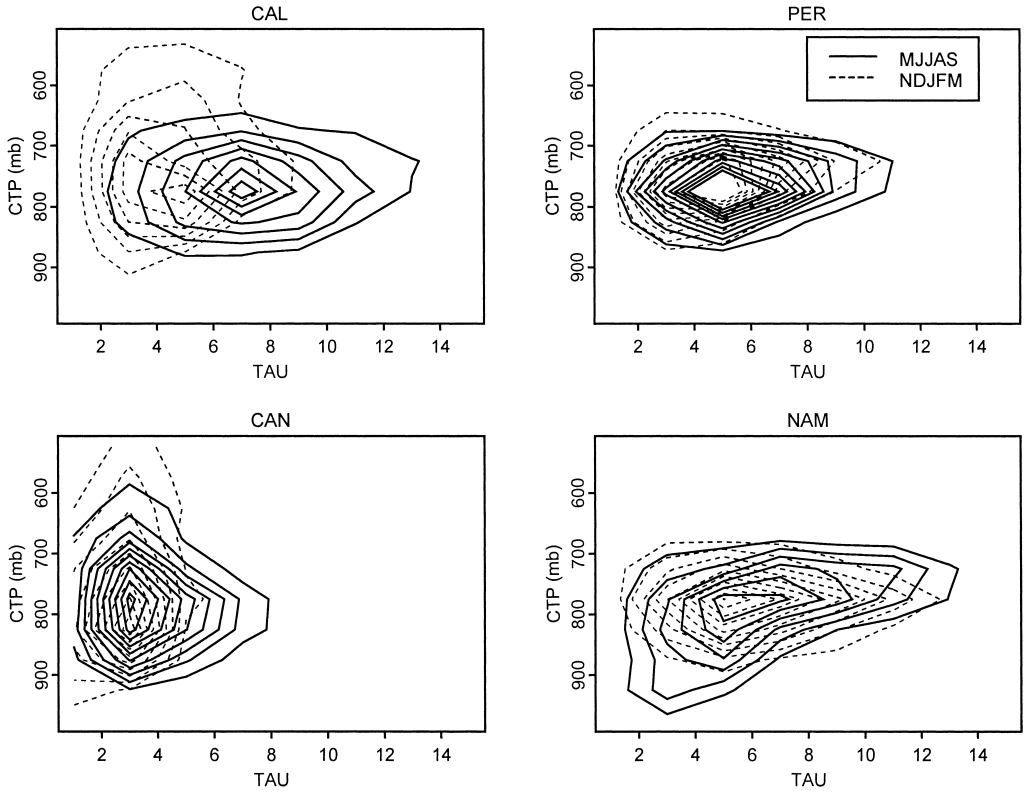

FIG. 5. 2D frequency distributions of daily average ISCCP total cloud TAU and CTP (1984–92) for the 10° × 10° domain. Solid lines are MJJAS and dotted lines are NDJFM. Contour lines are drawn for intervals of 20.

4. Intraseasonal variability of subtropical clouds and the general circulation during the NH winter

Thus far, studies of low-cloud fraction have found no single good predictor of submonthly cloud fraction variability. Correlations between low-cloud fraction and some large-scale meteorological factors on the synoptic timescale are examined by Wylie et al. (1989) for the First ISCCP Regional Experiment (FIRE) and by Klein (1997) during the MJJAS season at OSV *N*. These studies show increases in low-cloud fraction with increases in cold, dry advection, wind steadiness, latent heat flux, SLP, and surface divergence. However, the correlation coefficients are small, no larger than 0.35. In theory, an increase in cold, dry advection increases the sensible and latent heat fluxes between the relatively warm, moist ocean surface and the overlying air. An increase in surface wind speed also increases the magnitude of surface heat fluxes, and in addition, creates stronger wind shear, which increases the mechanical mixing in the near-surface boundary layer. One possible reason that these coefficients are so small is that the surface-observed cloud data are point measurements rather than truly synoptic in spatial scale. Increasing the size of the domain can increase the effective number of independent samples and decrease the standard error of the estimates if the region is large compared to spatial correlation lengths of a few thousand kilometers (Leith 1973).

However, if we repeat the calculations mentioned above and increase the spatial scale of the data by using ISCCP and ERA data on a 10° × 10° domain, the magnitude of the correlations coefficients does not increase. Klein et al. (1995), in their study of interannual variability, increase the correlation by lagging the time series by a day or two; this does not increase the coefficients in our case either Pincus et al. (1997) provides a complementary discussion using a Lagrangian rather than Eulerian framework, but again we find that either the coefficients are not larger than those mentioned previously, or they are not statistically significant.

Additionally, the weak correlations may arise from using cloud fraction as an indicator of cloud variability rather than TAU (which is directly related to cloud water) and CTP. It is much less clear how dynamical processes affect the horizontal distribution of cloud, than the production of cloud water and its distribution in the vertical. Unfortunately, in many datasets (e.g., OWS observations) cloud fraction is the only available cloud property.

In the following analysis, we examine the variability of clouds and meteorology together by compositing to study relationships between variables without making

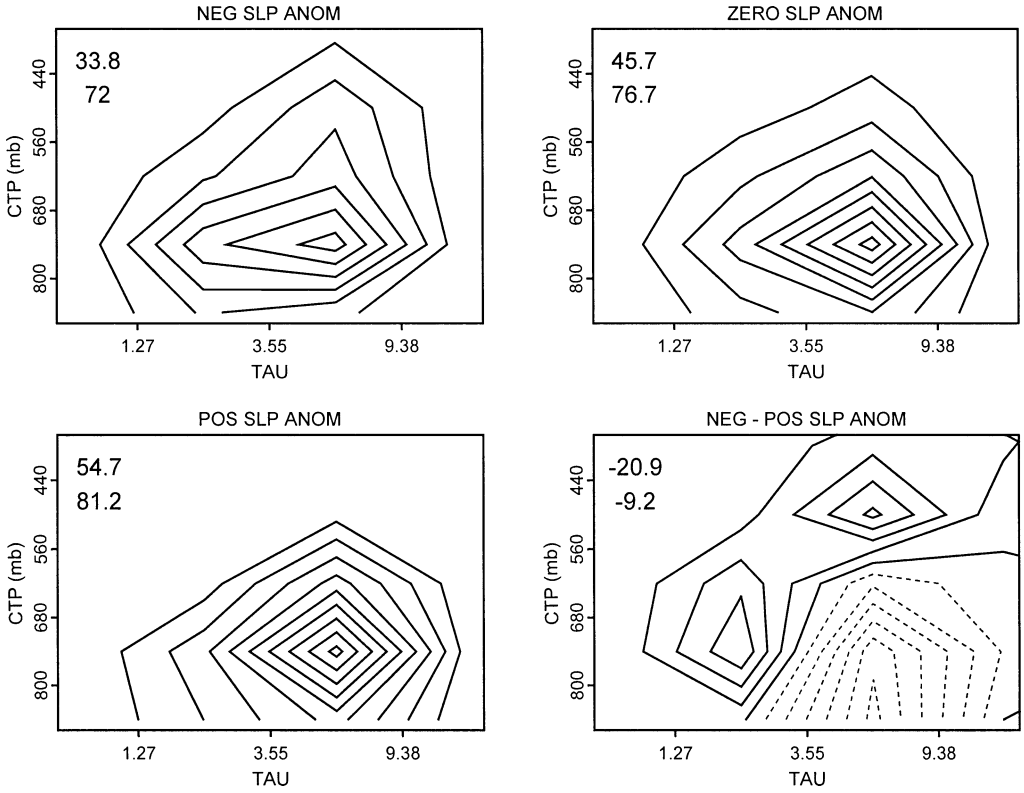

FIG. 6. 2D frequency distributions of daily average ISCCP total cloud TAU and CTP sorted by ERA seasonal SLP anomalies, CAL NDJFM (1984–90). Mean low- and total cloud fractions associated with each composite are printed in the upper left-hand corner. Contour lines are drawn for intervals of 4; the zero contour is labeled.

assumptions about the shapes of the frequency distributions. In the following sections we discuss selected variables in depth and summarize the remaining results.

a. Intraseasonal variability from ISCCP

We mentioned previously that changes in the intraseasonal variability of clouds in the NH from summer to winter indicate a change in dynamic regime with season, in particular, to variability associated with midlatitude synoptic waves. Following the examples of previous composite studies (Lau and Crane 1995, 1997; Tselioudis et al. 2000), we composite daily average cloud TAU and CTP based on the associated anomaly in SLP, and find that days of negative SLP anomaly (lower pressure) are associated more often with higher-altitude clouds and lower-altitude, thinner (smaller TAU) clouds in both NH regions (the Californian region is shown in Fig. 6). Unlike the studies mentioned above, these data are spatially averaged so the dispersion seen in these figures is due entirely to temporal variability.

We extend this analysis to include other variables (Table 4). Anomalies in ω_{700} divide subtropical cloud properties into smaller and larger CTP regimes (Fig. 7). Since ω_{700} is positive for descent and seasonally averaged ω_{700} is always positive, positive ω_{700} anomalies represent times of increased descent. In this figure, increased descent is associated with larger CTPs (or lower-

TABLE 4. Changes in composite cloud properties associated with positive anomalies in meteorology for the Californian and Canarian regions only during NDJFM. Cloud properties include low-cloud fraction (LCF), total cloud fraction (TCF), cloud optical thickness (TAU), and cloud-top pressure (CTP). Increases or decreases in cloud fraction are included if the amount exceeds 5%.

NDJFM variable	Change in cloud property			
	LCF	TCF	TAU	CTP
ERA SLP	Increase	Increase	Thicker	Larger
ERA Δ_vSLP	Decrease	Decrease	Thinner	None
ERA ω_{700}	Increase	Decrease	None	Larger
ERA θ_{1000}; ISCCP clear-sky temperature	Decrease	Decrease	Thinner	Smaller
ERA θ_{700}; ERA STAB	Increase	None	Thicker	Larger
STAB, TOVS θ_{740}	None	None	None	None

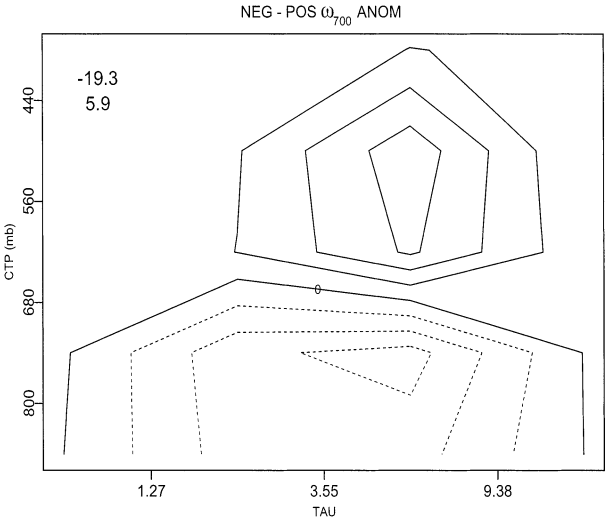

FIG. 7. Same as Fig. 6, but for anomalies in ERA ω_{700}.

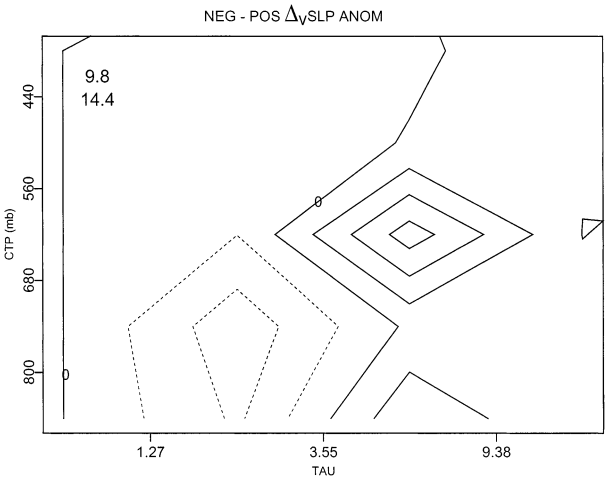

FIG. 8. Same as Fig. 6, but for anomalies in ERA Δ_vSLP.

altitude cloud tops). However, anomalies in ω_{700} have no apparent relationship to TAU variations.

As mentioned in the introduction, measuring the meteorological state of a single location is often not enough information to predict large-scale variability. For instance, during the large SLP phase of the synoptic wave, we noted that larger, positive SLP anomaly occupied most of the 2.5 boxes within our $10^\circ \times 10^\circ$ region. However, during the smaller SLP phase, the anomalies in the lower latitude boxes remained large and positive, while the higher latitude boxes showed smaller and negative SLP anomalies. Based on this, we felt that the progression of waves might be more apparent in a time series of the meridional gradient of SLP, rather than SLP alone. Figure 8 shows that thicker and thinner clouds at all altitudes are better separated by anomalies in the magnitude of Δ_vSLP across the region, a negative Δ_vSLP anomaly being associated with thicker clouds. A negative Δ_vSLP value occurs when the SLP on the poleward side of the box is larger than the equatorward side. Therefore, a negative Δ_vSLP anomaly occurs either when this gradient is large and negative or when the monthly mean meridional pressure gradient is larger and more positive than the daily value.

In order to separate clouds into two distinct CTP and TAU categories (or cloud types) at the same time, the cloud data are sorted by the Δ_vSLP and ω_{700} criteria together. Since correlations between seasonal anomalies of Δ_vSLP and ω_{700} are low in the NH subtropics during this season (r values of -0.1), we can sort the data using both criterion without redundancy. In Fig. 9, higher-altitude, thicker clouds are most often associated with negative anomalies in Δ_vSLP and ω_{700}. These tend to be times where Δ_vSLP is large and negative and upward ω_{700} (ascent). Lower-altitude, thinner clouds occur on days that have positive (smaller) values of Δ_vSLP and downward ω_{700}. The distribution using both criteria more closely resembles the ω_{700} distribution, with the Δ_vSLP criterion causing only slight shifts in the TAU categories.

These results are consistent with previous work. Some modeling studies have found a similar association between larger downward vertical velocities and larger CTPs (or thinner boundary layers), but until now no relationship to physical cloud thickness or TAU has been noted (e.g., Schubert et al. 1979; Hack et al. 1989; Philander et al. 1996). Analyses of synoptic waves in the NH midlatitude oceans have also found associations between the phase of the synoptic wave and changes in cloud properties (Lau and Crane 1995, 1997; Weaver and Ramanathan 1997; Weaver 1999; Norris and Klein 2000).

Although the anomalies mentioned above tended to group cloud properties in the most clearly defined categories, to a lesser extent we found relationships associated with other dynamic variables. For instance, we

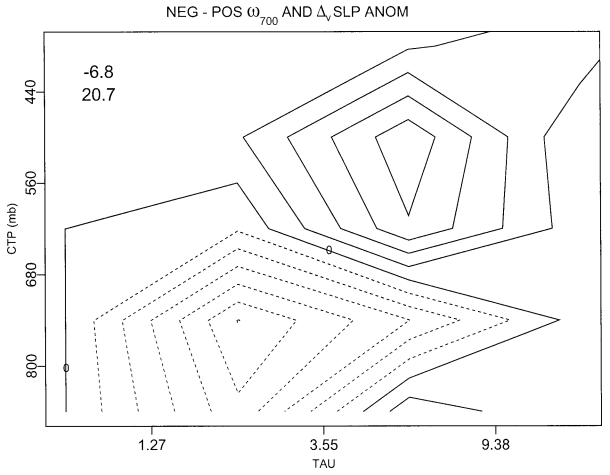

FIG. 9. Sorting ISCCP total cloud TAU and CTP by ERA ω_{700} and Δ_vSLP anomalies together during NDJFM (1984–90).

found smaller CTP clouds associated with stronger poleward wind speeds. We also found smaller CTP clouds associated temperature advection anomalies; warmer advection if the meridional wind direction was poleward, or less strong cold advection if it was equatorward.

These shifts in dynamic anomalies are also associated with anomalies in temperature alone. For instance, the combined criteria in Fig. 9 show that thicker, higher-altitude cloud tops tend to be associated with larger meridional SLP gradients and more negative (upward or less strong downward) ω_{700} anomalies. This is generally the warm sector of the synoptic storm, after the warm front passage and ahead of the cold front (e.g., Fig. 9 of Lau and Crane 1995). If we composite by surface temperature anomalies (using either ISCCP clear sky temperature or ERA θ_{1000}) we find that smaller CTP, thinner clouds are associated with warmer temperatures. This is consistent with the idea that higher altitude cloud tops are found in the warm sector of the synoptic wave.

However, compositing by the temperature above the boundary layer or by static stability provides results that are not so clear cut (results are summarized in Table 4). Static stability anomalies do not divide cloud properties into well-defined regimes in either region during this season. When taken separately, colder θ_{740} and surface temperature anomalies both appear to be weakly associated with thicker clouds. If a colder temperature anomaly is equal to a colder actual temperature, this is consistent with Tselioudis et al. (1992) and Tselioudis and Rossow (1994; although our study looks at the dynamically induced variations in temperature, while these studies examine the actual temperature dependence of TAU and how its sign changes with season and latitude while neglecting dynamically induced variations). If we composite the cloud data by actual stability and temperature values rather than seasonal anomalies, we find larger CTP and thicker clouds to be weakly associated with larger values of stability and colder θ_{740} and surface temperatures. The relationships between composited cloud properties and actual temperatures are stronger than in the seasonal anomaly case. Therefore, temperature may not be a good diagnostic for examining variability of cloud properties due to synoptic wave passage.

In an alternate analysis, we composited cloud properties using stability and temperature anomalies from ERA. In this case, positive anomalies in static stability are strongly associated with thicker, larger CTP clouds. ERA temperature anomalies associate thicker, larger CTP clouds with both warmer θ_{700} temperatures and colder θ_{1000} temperatures; therefore, both variables appear to be contributing to the relationship with ERA static stability. When we repeat the analysis using actual temperature values instead of anomalies, we find that ERA does show thicker clouds associated with larger values of stability and colder θ_{1000} temperatures, but we also find them associated with warmer θ_{700} temperatures, in disagreement with our results with TOVS and with Tselioudis et al. (1992).

Given what we know about both datasets, we cannot come to a definitive conclusion about the relationships seen here between static stability, temperature anomalies, and cloud properties. Addressing these discrepancies would involve cross-correlations between the temperature variables within each dataset and across the two datasets, plus an investigation into the causes of daily temperature variability in both datasets. While this subject is worth further investigation, we will not attempt to do so here.

In the NH regions, power spectra for static stability, surface temperature and θ_{740} (not shown) have a factor of 2 more power at seasonal to annual timescales (roughly 90 days to 1 yr) than cloud fraction, TAU, or CTP. In addition, these variables are autocorrelated for longer periods than cloud variables. Therefore, since temperature variables have more ''memory'' than cloud variables, their variability alone may not be a good proxy for submonthly low-cloud variability. Future research should include a study of which boundary layer variables (if any) exhibit temporal variability similar to the cloud properties.

b. Intraseasonal variability from surface observations

What does the passage of a synoptic wave do to the vertical structure of the subtropical boundary layer and thus to low clouds? In undisturbed conditions, the vertical structure consists of subcloud and cloudy layers capped vertically by a temperature inversion (sample soundings for the subtropical oceans are shown in Augstein et al. 1974; Schubert et al. 1979; Nicholls 1984; Albrecht et al. 1995b; Norris 1998; Weaver 1999). Since these layers are seldom well mixed, it is common to find profiles of q and θ_e decreasing with height, and θ increasing with height below the inversion.

As the synoptic wave passes, large-scale convergence, ascent and warming due to temperature advection occurs just preceding the low SLP anomaly (Lau and Crane 1995). As the air in the boundary layer is synoptically lifted, the entire subcloud layer cools at the adiabatic lapse rate. However, if q decreases with height, lower layers may reach saturation before upper layers and subsequently cool more slowly. This could destabilize the subcloud layer and cause vertical mixing. Nonuniform cooling can also destabilize the temperature inversion. Sarachik (1978) points out that large-scale lifting could cause the dry air above the inversion air to cool more rapidly than the cloudy air just below it, resulting in rapid instability and vertical mixing, which could temporarily wipe out the temperature inversion. Destabilization could also be caused by the horizontal advection of warmer air in beneath the cooler air, which is thought to be the dominant contribution to temperature changes in synoptic waves (Carlson 1991). All of these scenarios are consistent with data from OWS N

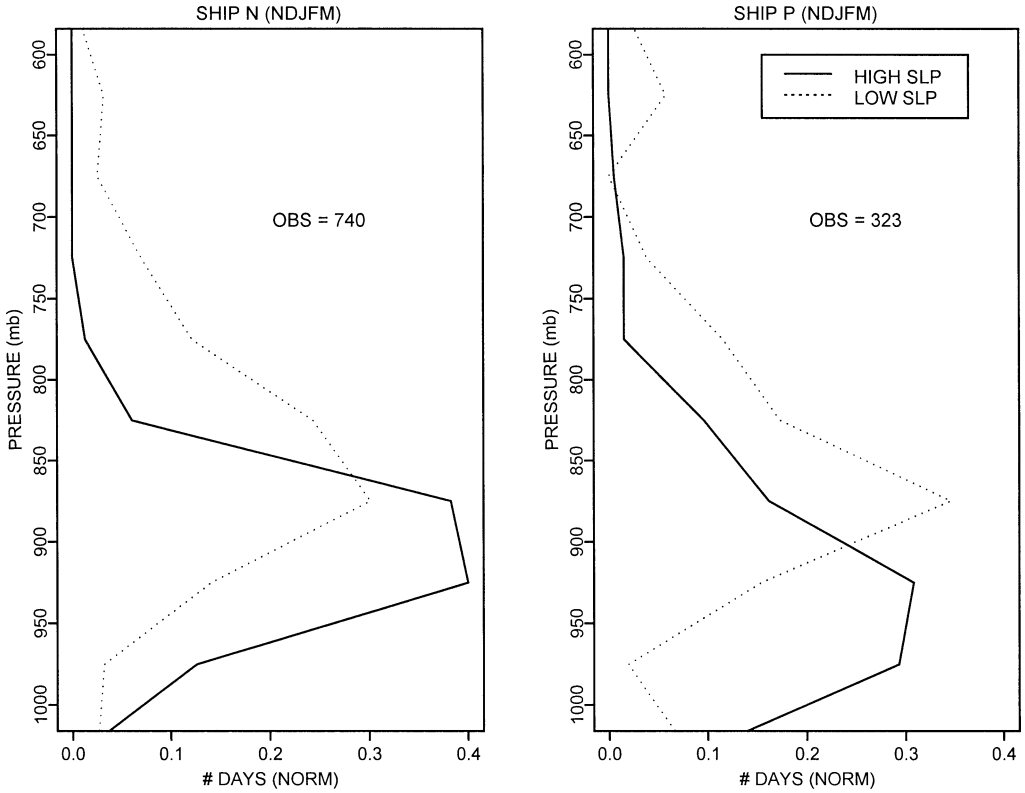

FIG. 10. Dependence of pressure at the base of the temperature inversion on SLP anomaly for NDJFM at (a) OWS N and (b) OWS P. The total number of soundings used in the frequency distribution is printed on the figure.

and OWS P, which show that wintertime soundings associated with anomalously low SLP more often have higher-altitude inversion heights or no inversion compared to soundings associated with positive SLP anomalies (Fig. 10 and Table 5). However, identifying the dominant influence is not possible from these point data.

This variation in inversion height in the subtropics with the phase of the synoptic wave provides a complementary picture to results shown by previous studies (Weaver 1999; Norris and Klein 2000) and obtained from ISCCP. Our results are a bit different for the following reasons. Norris and Klein (2000) examine the relationship between largescale subsidence and surface-observed cloud-type, not inversion height. Although it is implied by their study that St clouds are associated with lower-altitude inversion heights than Cu (Norris 1998), this is not shown explicitly, and we find this result without separating the clouds by their types. Weaver (1999) shows higher altitude inversion heights with *larger* values of subsidence (his Figs. 7 and 8). This result contradicts what we find for the subtropics. This discrepancy between results could be due to several reasons. For instance, Weaver composites surface data by actual large-scale subsidence rather than subsidence

TABLE 5. Mode, mean, and std dev of composite temperatures and pressures (in parentheses) for SLP anomalies during MJJAS and NDJFM. Californian region (CAL) pressures (mb) and temperatures (K) are those of the ISCCP cloud top; ocean weather station (OWS) pressures and temperatures are those associated with the base of the temperature inversion.

	POS SLP ANOM			NEG SLP ANOM		
Region	Mode	Mean	Std dev	Mode	Mean	Std dev
NDJFM						
CAL	279 (742)	276 (727)	7 (97)	285 (895)	271 (675)	11 (127)
OWS N	292 (825)	294 (828)	3 (43)	298 (825)	298 (804)	3 (53)
OWS P	282 (875)	283 (824)	4 (88)	287 (725)	286 (740)	12 (108)
MJJAS						
CAL	288 (755)	280 (736)	6 (75)	286 (773)	284 (781)	4 (62)
OWS N	296 (875)	296 (852)	3 (41)	300 (825)	300 (824)	3 (46)
OWS P	289 (875)	288 (882)	4 (62)	293 (775)	290 (805)	3 (63)

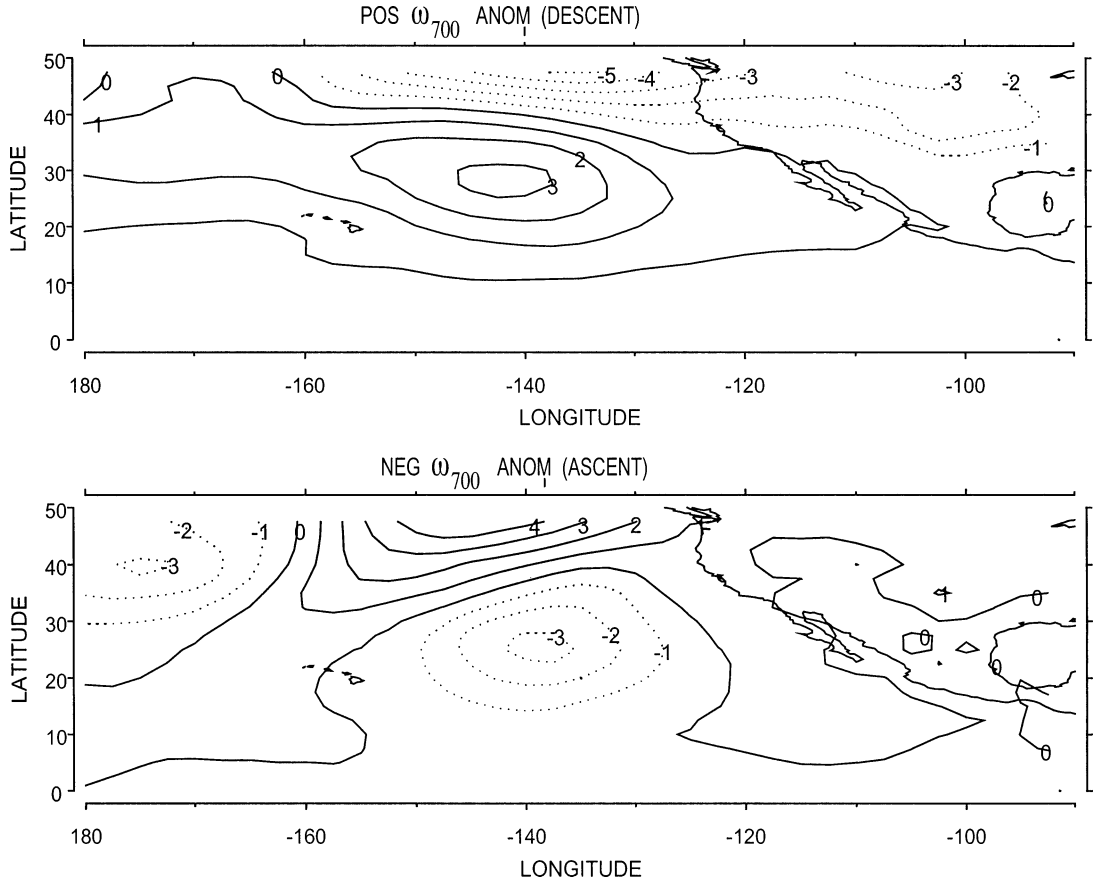

FIG. 11. Spatial pattern of composite SLP anomaly for NDJFM (1989–90) over the northern Pacific Ocean when ω_{700} anomalies in the 10° × 10° Californian region are (a) positive and (b) negative.

anomalies, thus implying in the discussion that any changes in subsidence from positive to negative is due to synoptic variability. In addition, Weaver speculates that deeper boundary layers are associated with cold front passages (and increasing subsidence) in the midlatitudes due to the larger turbulent fluxes generated as the colder air masses pass over a relatively warm ocean surface. Whether these discrepancies are due to different treatments of the data or to actual differences in processes (such as the dominance of subsidence effects in the subtropics over advective effects in the midlatitudes) should be the subject of future study.

5. Discussion

a. If the storm track did not intrude into the subtropical NH regions in winter, would low-cloud intraseasonal variability look similar to the summer season?

We cannot answer this question since the synoptic storms and their effects cannot be completely removed from the data. However, answering a related question may give us new insight. Given that most of the MJJAS intraseasonal variability exists under subsidence conditions, can the relationships found during MJJAS between clouds and meteorology be seen in the NDJFM during the increased subsidence phase of the wave?

For example, we found that the association between larger values of static stability, thicker clouds and larger low-cloud fraction is much stronger during the MJJAS season than during NDJFM. However, if we investigate a subset of the winter data, keeping only data where both the actual value of ω_{700} and the ω_{700} anomaly are positive, and we composite this subset by anomalies of stability, these NDJFM relationships become stronger. This result hints that if synoptic variability did not disturb the region, intraseasonal variability during winter would probably look similar to the summer case. In addition, Fig. 11a shows that when descent in the Californian region is anomalously large (downward), the spatial SLP anomaly pattern is largely zonal with high pressure dominating the subtropics. In the case where the ω_{700} anomaly is negative (Fig. 11b), the SLP anomaly pattern shows the synoptic wave structure with anomalous descent over the subtropics.

The interaction of synoptic variations in meteorology, cloud properties and underlying SSTs in the subtropics, adds a strongly nonlocal aspect to the problem of air–

sea interaction. The synoptic wave effects on cloud properties occur on a timescale of days and a spatial scale of thousand of kilometers. These waves are controlled by the large-scale structure of the local atmosphere but propagate in from much farther away. Although both the atmosphere and the ocean surface experience local changes in radiation and temperature on these scales, the oceanic response to these changes occurs more slowly than the atmospheric.

b. How could synoptic wave variability modulate subtropical cloud properties?

The correct way to address this question would be to use a cloud resolving model to analyze changes in cloud processes under conditions of synoptically varying large-scale forcing. This is the subject of current research, but we give a brief example of why these are important questions here. For instance, we observed in these data that changes in CTP are related to changes in large-scale subsidence. An increase in subsidence could increase CTP by mixing drier, warmer air into the upper layers of the cloud. This would presumably lower the altitude of the temperature and moisture inversions, which would in turn decrease the height to which buoyant parcels are transported from the ocean's surface. However, since boundary layer turbulence is driven primarily by radiative cooling and to a lesser extent by surface sensible and latent heat fluxes, and the strength of these processes are also altered during synoptic wave passage, the response will be complex and it is not certain which process will dominate.

6. Conclusions

We have explored the role of the general circulation in the large-scale variability of subtropical marine low-level cloud properties. Longer timescale processes change the basic state of the subtropics and the more rapid boundary layer processes at work within it. These interactions on different timescales make the variability nonlocal; this may account for the limited success of attempts to describe the system using only local, linear or single variable analyses.

The longer-period seasonal cycle plays a modulating role on daily to monthly variability. Seasonal differences in low-cloud fraction are found to be primarily due to changes in the mean values in the SH and to changes in frequency of occurrence and persistence in the NH. With the exception of the Canarian region, CTP–TAU frequency distributions indicate that these subtropical regions are more frequently populated by lower-altitude clouds with a wide range of optical thicknesses during the NH summer season. This pattern is altered during the winter season in the Californian region and during both seasons in the Canarian by large-scale synoptic variations in both cloud properties and meteorology. We have examined changes in cloud properties and meteorology as they occur together and have speculated that changes in cloud properties could be the result of changes in the large-scale circulation, but there is also reason to believe that the reverse can be true (e.g., Clark 1993). These differences highlight the difficulty of treating the seasonal cycle as decoupled from other timescales of variability. Our inability to consistently explain the seasonal variability in all four subtropical regions may be due in part to the fact that a portion of the apparent cycle (e.g., the minimum values of low-cloud fraction during the NDJFM season) occurs for different reasons in different locations. Since these subtropical regions do not appear to have the same type of variability, even for the large-amplitude forced mode of the seasonal cycle, there is a need for additional long-term observations of cloud and meteorology so that current theories on marine stratocumulus variability can be generalized to accommodate all regions. To add to this analysis, these data need to include simultaneous cloud property and meteorological data in both hemispheres, for both seasons, with sufficient resolution in cloud CTP and TAU.

A model such as Betts and Ridgway (1989), where cloud property changes in the subsidence regime are assumed to result from changes in tropical convection, cannot be used to test the larger amplitude variations induced by synoptic waves during the NH winter season since assumptions of continuous subsidence above the boundary layer and an equilibrium balance between the boundary layer and upper atmospheric parameters are violated in such a situation. This situation requires a smaller-scale model study that allows the large-scale conditions (such as subsidence, advective tendencies and surface heat fluxes) to vary in time and examines the effect of time varying large-scale circulation on cloud formation and dissipation processes. Simulating this case study may be more informative than the longer time period variability of the other seasons since the variability is larger in amplitude and the source of this variability is better understood. As we have demonstrated here, there are concerns about data quality; therefore, the main obstacle to testing these situations in models may be obtaining quality data to force them. These issues will be the subject of future work.

Acknowledgments. The authors would like to thank Drs. Brian Cairns, Ron Miller, and George Tselioudis for insightful comments during the progress of this work. Invaluable computer support was provided by Ralph Karow and Fabio Diniz. The detailed suggestions of three anonymous reviewers also substantially improved the paper. MAR is supported by a NASA GISS cooperative agreement NCCS-485 with the Department of Applied Physics at Columbia University.

REFERENCES

Albrecht, B. A., C. S. Bretherton, D. Johnson, W. H. Schubert, and A. S. Frisch, 1995a: The Atlantic Stratocumulus Transition Experiment—ASTEX. *Bull. Amer. Meteor. Soc.,* **76,** 889–904.

——, M. P. Jensen, and W. J. Syrett, 1995b: Marine boundary layer structure and fractional cloudiness. *J. Geophys. Res.,* **100,** 14 209–14 222.

Augstein, E., H. Schmidt, and F. Ostapoff, 1974: The vertical structure of the atmospheric planetary boundary layer in undisturbed trade winds over the Atlantic Ocean. *Bound.-Layer Meteor.,* **6,** 129–150.

Barker, H. W., 1996: A parameterization for computing grid-averaged solar fluxes for inhomogeneous marine boundary layer clouds. Part I: Methodology and homogeneous biases. *J. Atmos. Sci.,* **53,** 2289–2303.

Bechtold, P., S. K. Krueger, W. S. Lewellen, E. van Meijgaard, C.-H. Moeng, D. A. Randall, A. van Ulden, and S. Wang, 1996: Modeling a stratocumulus-topped PBL: Intercomparison among different 1D codes and with LES. *Bull. Amer. Meteor. Soc.,* **77,** 2033–2042.

Bergman, J., and M. Salby, 1996: Diurnal variations of cloud cover and their relationship to climatological conditions. *J. Climate,* **9,** 2802–2820.

Betts, A. K., 1990: Diurnal variation of California coastal stratocumulus from two days of boundary layer soundings. *Tellus,* **42A,** 302–304.

——, and W. Ridgway, 1989: Climatic equilibrium of the atmospheric convective boundary layer over a tropical ocean. *J. Atmos. Sci.,* **46,** 2621–2641.

Blaskovic, M., R. Davies, and J. B. Snider, 1991: Diurnal variation of marine stratocumulus over San Nicholas Island during July. *Mon. Wea. Rev.,* **119,** 1469–1478.

Bolton, D., 1980: The computation of equivalent potential temperature. *Mon. Wea. Rev.,* **108,** 1046–1053.

Bretherton, C. S., E. Klinker, A. K. Betts, and J. A. Coakley Jr., 1995: Comparison of ceilometer, satellite, and synoptic measurements of boundary-layer cloudiness and the ECMWF diagnostic cloud parameterization scheme during ASTEX. *J. Atmos. Sci.,* **52,** 2736–2751.

Burpee, R. W., 1972: The origin and structure of easterly waves in the lower troposphere of North Africa. *J. Atmos. Sci.,* **29,** 77–90.

Cairns, B., 1995: Diurnal variations of cloud from ISCCP data. *Atmos. Res.,* **37,** 133–146.

Carlson, T. N., 1969: Some remarks on African disturbances and their progress over the tropical Atlantic. *Mon. Wea. Rev.,* **97,** 716–726.

——, 1991: *Mid-Latitude Weather Systems.* Harper Collins Academic, 507 pp.

Chambers, L. H., B. A. Wielicki, and K. F. Evans, 1997: Independent pixel and two-dimensional estimates of Landsat-derived cloud field albedo. *J. Atmos. Sci.,* **54,** 1525–1532.

Chang, C.-P., 1970: Westward propagating cloud patterns in the tropical Pacific as seen from time-composite satellite photographs. *J. Atmos. Sci.,* **27,** 133–137.

Cho, H.-R., and Y. Ogura, 1974: A relationship between cloud activity and the low-level convergence as observed in Read-Recker's composite easterly waves. *J. Atmos. Sci.,* **31,** 2058–2065.

Clark, J. H. E., 1993: Radiatively driven interactions between stratocumulus and synoptic waves. *J. Atmos. Sci.,* **50,** 2731–2743.

Clement, A., and R. Seager, 1999: Climate and the tropical oceans. *J. Climate,* **12,** 3383–3401.

Del Genio, A. D., M.-S. Yao, W. Kovari, and K. K. W. Lo, 1996: A prognostic cloud water parameterization for global climate models. *J. Climate,* **9,** 270–304.

Gilman, D. L., F. J. Fuglister, and J. M. Mitchell Jr., 1963: On the power spectrum of ''red noise.'' *J. Atmos. Sci.,* **20,** 182–184.

Gordon, C. T., A. Rosati, and R. Gudgel, 2000: Tropical sensitivity of a coupled model to specified ISCCP low clouds. *J. Climate,* **13,** 2239–2260.

Hack, J. J., W. H. Schubert, D. E. Stevens, and H.-C. Kuo, 1989: Response of the Hadley circulation to convective forcing in the ITCZ. *J. Atmos. Sci.,* **46,** 2957–2973.

Hahn, C. J., W. B. Rossow, and S. G. Warren, 2001: ISCCP cloud properties associated with standard cloud types identified in individual surface observations. *J. Climate,* **14,** 11–28.

Han, Q., W. B. Rossow, J. Chou, and R. M. Welch, 1998: Global survey of the relationships of cloud albedo and liquid water path with droplet size using ISCCP. *J. Climate,* **11,** 1516–1528.

Jakob, C., 1999: Cloud cover in the ECMWF reanalysis. *J. Climate,* **12,** 947–959.

Jin, Y., and W. B. Rossow, 1997: Detection of overlapping low-level clouds. *J. Geophys. Res.,* **102,** 1727–1737.

Klein, S. A., 1997: Synoptic variability of low-cloud properties and meteorological parameters in the subtropical trade wind boundary layer. *J. Climate,* **10,** 2018–2039.

——, and D. L. Hartmann, 1993: The seasonal cycle of low stratiform clouds. *J. Climate,* **6,** 1587–1606.

——, ——, and J. R. Norris, 1995: On the relationships among low cloud structure, sea surface temperature, and atmospheric circulation in the summertime northeast Pacific. *J. Climate,* **8,** 1140–1155.

Larson, K., D. L. Hartmann, and S. A. Klein, 1999: The role of clouds, water vapor, circulation, and boundary layer structure in the sensitivity of the tropical climate. *J. Climate,* **12,** 2359–2374.

Lau, N.-C., and M. W. Crane, 1995: A satellite view of the synoptic-scale organization of cloud properties in midlatitude and tropical circulation systems. *Mon. Wea. Rev.,* **123,** 1984–2006.

——, and ——, 1997: Comparing satellite and surface observations of cloud patterns in synoptic-scale circulation systems. *Mon. Wea. Rev.,* **125,** 3172–3189.

Leith, C. E., 1973: The standard error of time-average estimates of climatic means. *J. Appl. Meteor.,* **12,** 1066–1069.

Li, J.-F., M. Kohler, and C. R. Mechoso, 2000: The impact of improved stratocumulus cloud optical properties on a general circulation model. *Proc. 13th Int. Conf. on Clouds and Precipitation,* Reno, NV, International Committee on Clouds and Precipitation, Vol. 2, 311–314.

Ma, C.-C., C. R. Mechoso, A. W. Robertson, and A. Arakawa, 1996: Peruvian stratus clouds and the tropical Pacific circulation: A coupled ocean–atmosphere GCM study. *J. Climate,* **9,** 1635–1645.

Miller, R., 1997: Tropical thermostats and low cloud cover. *J. Climate,* **10,** 409–440.

Moeng, C.-H., and Coauthors, 1996: Simulation of a stratocumulus-topped planetary boundary layer: Intercomparison among different numerical codes. *Bull. Amer. Meteor. Soc.,* **77,** 261–278.

Nicholls, S., 1984: The dynamics of stratocumulus: Aircraft observations and comparisons with a mixed layer model. *Quart. J. Roy. Meteor. Soc.,* **110,** 783–820.

Norris, J. R., 1998: Low cloud type over the ocean from surface observations. Part I: Relationship to surface meteorology and the vertical distribution of temperature and moisture. *J. Climate,* **11,** 369–382.

——, and S. A. Klein, 2000: Low cloud type over the ocean from surface observations. Part III: Relationship to vertical motion and the regional surface synoptic environment. *J. Climate,* **13,** 245–256.

Pandolfo, L., 1993: Observational aspects of the low-frequency intraseasonal variability of the atmosphere in middle latitudes. *Advances in Geophysics,* Vol. 34, Academic Press, 93–174.

Peixoto, J. P., and A. H. Oort, 1992: *The Physics of Climate.* American Institute of Physics, 520 pp.

Philander, S. G. H., D. Gu, D. Halpern, G. Lambert, N.-C. Lau, T. Li, and R. C. Pacanowski, 1996: Why the ITCZ is mostly north of the equator. *J. Climate,* **9,** 2958–2972.

Pincus, R., M. B. Baker, and C. S. Bretherton, 1997: What controls stratocumulus radiative properties? Lagrangian observations of cloud evolution. *J. Atmos. Sci.,* **54,** 2215–2236.

Press, W. H., Ed.,1992: *Numerical Recipes in Fortran.* Cambridge University Press, 963 pp.

Randall, D. A., B. Albrecht, S. Cox, D. Johnson, P. Minnis, W. Rossow, and D. O'C. Starr, 1996: On FIRE at ten. *Advances in Geophysics,* Vol. 38, Academic Press, 37–177.

Reed, R. J., D. C. Norquist, and E. E. Recker, 1977: The structure and properties of African wave disturbances as observed during Phase III of GATE. *Mon. Wea. Rev.,* **105,** 317–333.

Rossow, W. B., and B. Cairns, 1995: Monitoring changes of clouds. *Climatic Change,* **31,** 305–347.

——, and R. A. Schiffer, 1999: Advances in understanding clouds from ISCCP. *Bull. Amer. Meteor. Soc.,* **80,** 2261–2287.

——, A. W. Walker, and L. C. Garder, 1993: Comparison of ISCCP and other cloud amounts. *J. Climate,* **6,** 2394–2418.

——, ——, D. E. Beuschel, and M. D. Roiter, 1996: International Satellite Cloud Climatology Project (ISCCP) description of new cloud datasets. WMO Tech. Doc. 737, World Climate Research Programme, ICSU and WMO, 115 pp.

Rozendaal, M. A., C. B. Leovy, and S. A. Klein, 1995: An observational study of diurnal variations of marine stratiform cloud. *J. Climate,* **8,** 1795–1809.

Salby, M. L., 1996: *Fundamentals of Atmospheric Physics.* Academic Press, 627 pp.

Sarachik, E., 1978: Tropical sea surface temperature: An interactive one-dimensional atmosphere–ocean model. *Dyn. Atmos. Oceans,* **2,** 455–469.

Schubert, W. H., J. S. Wakefield, E. J. Steiner, and S. K. Cox, 1979: Marine stratocumulus convection. Part I: Governing equations and horizontally homogeneous solutions. *J. Atmos. Sci.,* **36,** 1286–1307.

Sengupta, S. K., R. M. Welch, M. S. Navar, T. A. Berendes, and D. W. Chen, 1990: Cumulus cloud field morphology and spatial patterns derived from high spatial resolution Landsat imagery. *J. Appl. Meteor.,* **29,** 1245–1267.

Simon, R. L., 1977: The summertime stratus over the offshore waters of California. *Mon. Wea. Rev.,* **105,** 1310–1314.

Stubenrauch, C. J., W. B. Rossow, F. Cheruy, A. Chedin, and N. A. Scott, 1999: Clouds as seen by satellite sounders (3I) and imagers (ISCCP). Part I: Evaluation of cloud parameters. *J. Climate,* **12,** 2189–2213.

Trenberth, K., 1991: Storm tracks in the Southern Hemisphere. *J. Atmos. Sci.,* **48,** 2159–2178.

Tselioudis, G., and W. B. Rossow, 1994: Global, multiyear variations of optical thickness with temperature in low and cirrus clouds. *Geophys. Res. Lett.,* **21,** 2211–2214.

——, ——, and D. Rind, 1992: Global patterns of cloud optical thickness variation with temperature. *J. Climate,* **5,** 1484–1495.

——, Y.-C. Zhang, and W. B. Rossow, 2000: Cloud and radiation variations associated with northern midlatitude low and high sea level pressure regimes. *J. Climate,* **13,** 312–327.

Wang, J., W. B. Rossow, T. Uttal, and M. Rozendaal, 1999: Variability of cloud vertical structure during ASTEX observed from a combination of rawinsonde, radar, ceilometer and satellite. *Mon. Wea. Rev.,* **127,** 2484–2502.

Warren, S. G., C. J. Hahn, J. London, R. M. Chevin, and R. L. Jenne, 1988: Global distribution of total cloud cover and cloud type amounts over the ocean. NCAR Tech. Note 317+STR, 42 pp. and 170 maps.

Weaver, C. J., and R. Pearson Jr., 1990: Entrainment instability and vertical motion as causes of stratocumulus breakup. *Quart. J. Roy. Meteor. Soc.,* **116,** 1359–1388.

Weaver, C. P., 1999: The interactions among cyclone dynamics, vertical thermodynamics structure, and cloud radiative forcing in the North Atlantic summertime storm track. *J. Climate,* **12,** 2625–2642.

——, and V. Ramanathan, 1997: Relationships between large-scale vertical velocity, static stability, and cloud radiative forcing over Northern Hemisphere extratropical oceans. *J. Climate,* **10,** 2871–2887.

Webb, M., C. A. Senior, S. Bony, and J.-J. Morcrette, 2001: Combining ERBE and ISCCP data to assess clouds in the Hadley Centre, ECMWF and LMD atmospheric climate models. *Climate Dyn.,* **17,** 905–922.

Welch, R. M., K. S. Kuo, B. A. Wielicki, S. K. Sengupta, and L. Parker, 1988: Marine stratocumulus cloud fields off the coast of southern California observed using LANDSAT imagery. Part I: Structural characteristics. *J. Appl. Meteor.,* **27,** 341–362.

Wylie, D., B. B. Hinton, and K. Kloesel, 1989: The relationship of marine stratus clouds to wind and temperature advection. *Mon. Wea. Rev.,* **117,** 2620–2625.

Yu, J.-Y., and C. R. Mechoso, 1999: Links between annual variations of Peruvian stratocumulus clouds and of SST in the eastern equatorial Pacific. *J. Climate,* **12,** 3305–3318.